Available online at www.sciencedirect.com
SCIENCE DIRECT
Polymer 47 (2006) 2839–2848
polymer
www.elsevier.com/locate/polymer

X-ray studies of regenerated cellulose fibers wet spun from cotton linter pulp in NaOH/thiourea aqueous solutions

Xuming Chen [a], Christian Burger [a], Dufei Fang [a], Dong Ruan [b], Lina Zhang [b], Benjamin S. Hsiao [a,*], Benjamin Chu [a,**]

[a] *Department of Chemistry, Stony Brook University, Stony Brook, NY 11794-3400, USA*
[b] *Department of Chemistry, Wuhan University, Wuhan 430072, China*

Received 13 December 2005; received in revised form 13 February 2006; accepted 14 February 2006
Available online 10 March 2006

Abstract

Regenerated cellulose fibers were fabricated by dissolution of cotton linter pulp in NaOH (9.5 wt%) and thiourea (4.5 wt%) aqueous solution followed by wet-spinning and multi-roller drawing. The multi-roller drawing process involved three stages: coagulation (I), coagulation (II) and post-treatment (III). The crystalline structure and morphology of regenerated cellulose fiber was investigated by synchrotron wide-angle X-ray diffraction (WAXD) and small-angle X-ray scattering (SAXS) techniques. Results indicated that only the cellulose II crystal structure was found in regenerated cellulose fibers, proving that the cellulose crystals were completely transformed from cellulose I to II structure during spinning from NaOH/thiourea aqueous solution. The crystallinity, orientation and crystal size at each stage were determined from the WAXD analysis. Drawing of cellulose fibers in the coagulation (II) bath (H_2SO_4/H_2O) was found to generate higher orientation and crystallinity than drawing in the post-treatment (III). Although the post-treatment process also increased crystal orientation, it led to a decrease in crystallinity with notable reduction in the anisotropic fraction. Compared with commercial rayon fibers fabricated by the viscose process, the regenerated cellulose fibers exhibited higher crystallinity but lower crystal orientation. SAXS results revealed a clear scattering maximum along the meridian direction in all regenerated cellulose fibers, indicating the formation of lamellar structure during spinning.

Keywords: Cellulose fibers; Cotton linter; Thiourea

1. Introduction

Cellulose is the most abundant renewable organic material on earth. It exhibits unique physical and mechanical properties that are useful in many applications. However, the regeneration of cellulose fiber has always been a challenging problem because of the many environmental issues related to the existing processes [1,2]. The problem is mainly due to the characteristics of cellulose crystal structures that cannot be melt processed (the degradation temperature is lower than the melting temperature) or solution processed in common solvents (due to the presence of strong hydrogen bonding in the crystals).

The oldest technology for producing regenerated cellulose fibers (e.g. rayon fibers) is the viscose process that was developed over 100 years ago [1,2]. This process, unfortunately, also generates several environmentally hazardous byproducts, including CS_2, H_2S and heavy metals [3]. The cuprammonium process is an alternative route to produce regenerated cellulose fibers (cupro silk, cuprophane). However, it also has environmental problems and has only been practiced scarcely in the industry [1]. Throughout the years, many other alternative methods have been developed to reduce the processing steps as well as to minimize the hazardous byproducts. For example, the *N*-methylmorpholine-*N*-oxide (NMMO) process has become a more desirable method over the dominating viscose process because it produces less hazardous byproducts. However, the fibers produced by the NMMO process (or the Lyocell process), although being of high strength with good stability, also display a high fibrillation tendency in the wet state. These properties can be attributed to the high degree of crystallinity and high orientation of cellulose chains in the non-crystalline regions in the fiber. The Lyocell process still has many environmental issues that need to be

* Corresponding authors. Tel.: +1 631 632 7793.
** Tel.: +1 631 632 7928; fax: +1 631 632 6518.
E-mail addresses: bhsiao@notes.cc.sunysb.edu (B.S. Hsiao), bchu@notes.cc.sunysb.edu (B. Chu).

0032-3861/$ - see front matter © 2006 Elsevier Ltd. All rights reserved.
doi:10.1016/j.polymer.2006.02.044

overcome for the efficient and environment-friendly production of cellulose fibers. These issues include the minimization of several side reactions, further reduction of undesired byproducts and efficient recovery of the expensive solvent [4].

Recently, a series of new solvents, such as NaOH/urea and NaOH/thiourea aqueous systems for dissolution of cotton linter pulp cellulose have been developed by the research group of the co-author in Wuhan University in China [5–16]. The properties of these cellulose solutions and resulting fibers/films have been investigated to some extent. For example, the ^{13}C NMR analysis showed that these solvents and cellulose formed a non-derivative aqueous solution system [7,8]. The presence of urea (orthiourea) significantly enhanced the solubility of cellulose in NaOH aqueous solution and reduced the formation of cellulose gel [11]. Regenerated cellulose fibers wet-spun from NaOH/thiourea aqueous solutions exhibited round cross-sections with properties similar to those of natural silk (e.g. good flexibility and luster), but different from the viscose rayon fiber that usually exhibits irregular cross-sections [7a]. The physical properties of the fibers produced by the NaOH/urea (thiourea) methods are close to those of the fibers by the NMMO process, owing to the similar dissolution and regeneration conditions in spinning [7]. The lower cost and less toxicity of the NaOH/urea (thiourea) solvent system, and its relative ease for wet spinning exhibited some good promises for the development of a more economical and environment-friendly process for regeneration of cellulose fibers. However, as this solvent system is relatively new, its wet spinning process has still not been fully optimized.

The crystalline structure of cellulose was investigated almost a century ago by Nishikawa and Ono based on fiber bundles from various plants [17], and has been a matter of active debate since then, mostly due to the difficulties of separating the mixture of cellulose I_α and I_β occurring in all forms of native cellulose. Following the success of these experiments, X-ray diffraction was widely used for studying both natural and regenerated cellulose fibers by different processes [18,19]. In this study, the relationships between the wet spinning process, the structure and properties of cellulose fibers generated from a cotton linter pulp in NaOH/thiourea aqueous solution have been investigated. The regenerated cellulose fibers wet spun from another similar solvent system (i.e. NaOH/urea aqueous solution) will be discussed elsewhere. The state of aggregation for cellulose in NaOH/thiourea aqueous solution has first been investigated by dynamic light scattering (DLS). The structural changes in crystal and amorphous regions, as well as in chain orientation during varying processing stages and draw conditions from the cotton and NaOH/thiourea aqueous solution have subsequently been characterized by combined wide-angle X-ray diffraction (WAXD) and small-angle X-ray scattering (SAXS) techniques with synchrotron radiation. The small beam divergence and the high brilliance of synchrotron X-rays permit measurements with small sample specimens and high spatial resolution [20] and the use of simultaneous SAXS/WAXD has been shown to be a particularly powerful tool for investigating the crystal structure and orientation in oriented polymer materials during processes in real time [20–28]. Results indicated some possible pathways for improving the wet-spinning process of the cellulose in NaOH/thiourea aqueous solution.

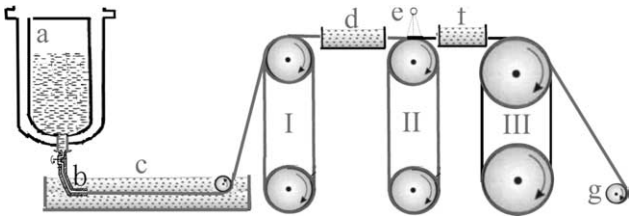

Fig. 1. Schematic diagram of the pilot scale spinning machine: (a) a pressure extrude with a stainless cylinder having cooling jacket; (b) filter and spinneret; (c) first coagulation bath; (d) second coagulation bath; (e) hot water washing; (f) third post-treatment bath (plasticizing bath); (g) take-up device; (I) Nelson-type roller; (II) Nelson-type roller; (III) heated roller. First coagulation bath: 10 wt% NH_4Cl and 4 wt% H_2SO_4 in aqueous solution; second coagulation bath: 5 wt% H_2SO_4 in aqueous solution.

2. Experimental

The regeneration of cellulose fibers, wet-spun from cotton linter pulp (degree of polymerization, DP ~ 550, Hubei Chemical Fiber Co. Ltd, China) in NaOH (9.5 wt%)/thiourea (4.5 wt%) aqueous solution, has been demonstrated by Zhang et al. in Wuhan University in China before [5–16]. The chosen sample preparation and processing schemes in this study were similar to those demonstrated earlier [7a–c]. In brief, cotton linter pulp was first dissolved in the NaOH/thiourea aqueous solvent to prepare the cellulose solution. The wet spinning process was carried out by a lab-scale spinning apparatus. The schematic diagram of this apparatus is shown in Fig. 1, where the wet spinning conditions are listed in Table 1. The wet spinning process was coupled with drawing stages after treatments in three different baths: coagulation (I), coagulation (II) and post-treatment (III). The samples after each processing step were collected for X-ray study. Two types of commercial viscose rayon fibers (Hubei Chemical Fiber Co. Ltd, China) were also measured for comparison.

Synchrotron wide-angle X-ray diffraction (WAXD) and small-angle X-ray scattering (SAXS) experiments were carried out at the advanced polymers beamline (X27C) in the National Synchrotron Light Source (NSLS), Brookhaven National Laboratory (BNL). The details of the experimental setup at the X27C beamline have been reported elsewhere [20]. The wavelength used was 0.1371 nm. A three-pinhole collimation system was used to define the incident beam from a double

Table 1
Wet spinning speed and spin draw ratio (SDR) chosen for regeneration of cellulose fibers in this study

Sample ID	Flow speed at spinnet (m/min)	ν_I (m/min)/ SDR_I	ν_{II} (m/min)/ SDR_{II}	ν_{III} (m/min)/ SDR_{III}
S1	84.9	30.13/0.35	–	–
S2	84.9	30.13/0.35	32.61/1.08	–
S3	84.9	30.13/0.35	32.61/1.08	34.31/1.05
S4	84.9	30.13/0.35	34.25/1.14	34.98/1.02

multi-layered monochromator. A bundle of cellulose fibers (about 60 parallel filaments, the diameter of the single regenerated cellulose fiber was about 20–30 μm) were placed in a sample holder with the fiber direction perpendicular to the X-ray beam. The sample-to-detector distance was 108.4 mm for WAXD and 1802.6 mm for SAXS, respectively. A 2D MAR–CCD (MAR USA, Inc.) X-ray detector was used for the data collection. A typical image acquisition time was 45 s.

2D WAXD patterns were corrected for air scattering and incident beam intensity fluctuations, as well as for the effects of the curvature of the Ewald sphere (Fraser correction [29]). The crystallinity was estimated from the WAXD pattern using the following procedures. The integrated diffraction intensity profile was first calculated from the Fraser corrected WAXD patterns. Individual crystal reflection peaks and the amorphous background were extracted by the curve-fitting process of the integrated diffraction intensity profile. The crystallinity was estimated as the ratio of the total crystal peak intensity to the total diffraction intensity.

The orientation of the cellulose fiber was analyzed by using the following method. Assuming that the cellulose crystallites were oriented around the fiber axis (we assumed that the polymer chain axis was identical to the crystallographic c-axis), the crystal orientation could be characterized by an orientation distribution function $g(\beta)$ with β being the azimuthal angle defined as zero at the meridian. As a probability density distribution, $g(\beta)$ is positive over its entire range. Its normalization can be given by $\int_0^{\pi/2} g(\beta)\sin\beta \mathrm{d}\beta = 1$. The limited integration angle reflects the symmetry conditions imposed by the combination of cylindrical and inversion symmetry. Assuming that the orientation distribution function $g(\beta)$ is well behaved and unimodally peaked around $\beta = 0$, a single parameter characterizing the degree of preferred orientation is the Hermans' orientation parameter

$$\bar{P}_{2,g} = (3/2)\int_0^{\pi/2} \cos^2\beta g\beta \sin\beta \mathrm{d}\beta - 1/2$$

where $\bar{P}_2$ represents the average over a Legendre polynomial of the second order. The $\bar{P}_{2,g}$ of the orientation distribution $g(\beta)$ will vary from 0 for completely isotropic systems to 1 for perfectly oriented systems. The azimuthal component of experimental peak profiles could, after normalization, also be used to calculate $\bar{P}_{2,g}$. For a meridional peak (and under certain approximate assumptions, which would be well fulfilled in this case), $\bar{P}_{2,g} = \bar{P}_{2,\mathrm{mer}}$. However, as the cellulose crystal does not show any significant meridional peaks, if an equatorial peak is considered, the relationship becomes $\bar{P}_{2,g} = -2\bar{P}_{2,\mathrm{eq}}$. The $\bar{P}_{2,\mathrm{eq}}$ value of a perfectly well oriented equatorial peak would then be $-1/2$.

Dynamic light scattering (DLS) measurements of cellulose in NaOH/thiourea aqueous solution was also carried out to investigate the nature of polymer chain in solution and to correlate with the X-ray results from fibers. The solution was prepared by dissolving ~0.1 wt% cotton linter pulp (DP ~ 550) into NaOH (9.5 wt%)/thiourea (4.5 wt%) aqueous solution using the following procedure [7]. The solvent system, NaOH/thiourea aqueous solution, was first pre-cooled to −8 °C. Then 0.1 g of cotton linter pulp was added to 100 ml solvent under vigorous stirring at ambient temperature for 5 min to obtain a clear cellulose solution. The solution was then filtered through an M-size glass filter and then kept in a refrigerator (~5 °C) for at least 2 days. A stoichiometric amount of 1 M HCl was used to neutralize the NaOH component and to precipitate the cellulose in 30 ml of the above solution. The exact concentration of the cellulose in NaOH (9.5 wt%)/thiourea (4.5 wt%) aqueous solution was determined from the weight of the precipitated cellulose.

A standard laboratory-built laser light scattering (LLS) instrument equipped with a BI-9000 AT digital correlator and a solid-state laser (DPSS, coherent, 200 mW, 532 nm) was used to perform DLS measurement. The CONTIN program [30] was used for the data analysis of intensity–intensity time correlation functions. After knowing the translational diffusion coefficient D, the apparent hydrodynamic radius R_h was calculated by using the Stokes–Einstein relation: $R_h = k_B T/(6\pi\eta D)$, where k_B, T, and η are the Boltzmann constant, the absolute temperature, and the solvent viscosity, respectively.

3. Results and discussion

3.1. WAXD results

A typical 2D WAXD pattern of sample S3 (corresponding processing conditions are listed in Table 1) is shown in Fig. 2, in which all reflection peaks can be indexed based on the known cellulose II crystal structure. Compared with the 2D WAXD pattern of the original cotton linter pulp (Fig. 3), which shows cellulose I structure, the regenerated S3 fiber only exhibits the cellulose II structure. This indicates that the cellulose I structure in cotton linter pulp was completely converted to the cellulose II structure after spinning from the NaOH/thiourea solution. The chain conformation and packing of crystalline allomorphs of various celluloses has been described by Zugenmaier [31]. The structure of cellulose II consists of two anti-parallel and crystallographically independent chains [32,33], arranged in a monoclinic cell, where the

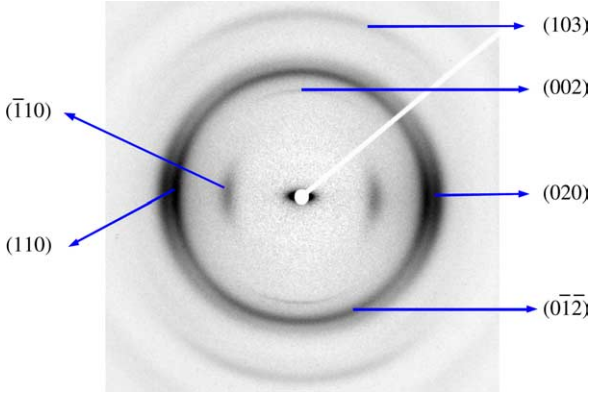

Fig. 2. Typical 2D WAXD pattern of the regenerated cellulose fiber (S3); corresponding reflection peaks were indexed by the cellulose II structure.

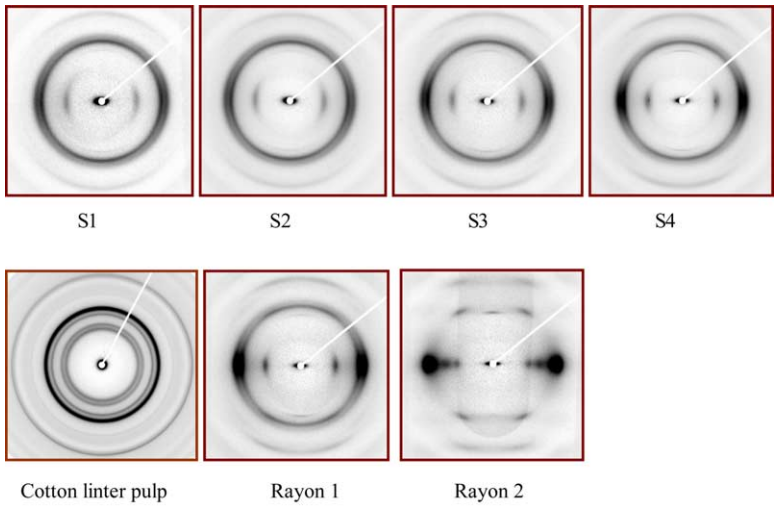

Fig. 3. 2D WAXD patterns of the cellulose fibers wet spun from the NaOH/thirourea aqueous solution using different processing conditions and two commercially available rayon fibers.

chains are aligned with the two-fold screw axis of the cell. Although both chains have same backbone conformations, however, they have different conformation in their hydroxymethyl groups. The glycosyl residues have the gauche–trans conformation, when they are located at the origin of the unit cell, or trans-gauche conformation for those of the center chain. However, with the investigations by using ^{13}C NMR spectroscopy [34,35] and the determination of crystalline structure of β-cellotetraose hemihydrate [36,37], the above cellulose II structure has been under dispute. Both chains have equivalent backbone conformations but differ in the conformation of their hydroxymethyl groups. These moieties are near the gauche–trans conformation for the glycosyl residues located at the origin of the unit cell as opposed to the tg conformation for those of the center chain. However, this cellulose II structure has been challenged by the observations from a number of ^{13}C NMR spectroscopy studies [34,35] and by the determination of the crystalline structure of β-cellotetraose hemihydrate [36,37], which adopts a crystalline packing almost equivalent to that of cellulose II. On the basis of high-resolution synchrotron X-ray data collected from ramie fibers, Langan et al. refined the monoclinic structure for cellulose II, leading to the unit cell parameters $a=8.10$ Å, $b=9.03$ Å, $c=10.31$ Å, and $\gamma=117.1°$ [38], the peak assignments in Fig. 2 were based upon. Fig. 2 shows that the reflections of (110), ($\bar{1}10$) and (020) are located on the equator while the other reflections are found at off-axis positions, indicating that cellulose II was preferentially oriented with its crystallographic *c*-axis pointing along the fiber direction.

Fig. 3 shows 2D WAXD patterns of all regenerated cellulose fiber samples created in this study, the original cotton linter pulp and the two commercial rayon samples. It is seen that, except for the original cotton linter pulp sample that exhibits the cellulose I structure, all other samples exhibit the cellulose II structure. This indicates that the dissolution processes (by NaOH/thiourea or viscose) can only generate cellulose II. WAXD patterns of the four new regenerated cellulose fibers were very similar. All reflections appeared as broad arcs, indicating the existence of moderate crystal orientation. However, the reflections of two commercial rayon fibers, short arcs in rayon 1 and sharp spots in rayon 2, indicate a very high degree of orientation of cellulose II crystals in those samples. For the WAXD pattern of rayon 2, we observed a peak located between ($\bar{1}10$) and (110). This peak might be due to the diffraction of some additive, which is unknown to us. However, the observed WAXD pattern from rayon 2 clearly showed the cellulose II structure.

The procedure for estimation of the crystallinity and crystal size from the WAXD data is illustrated in Fig. 4. In this procedure, the 1D intensity profile was obtained by integration

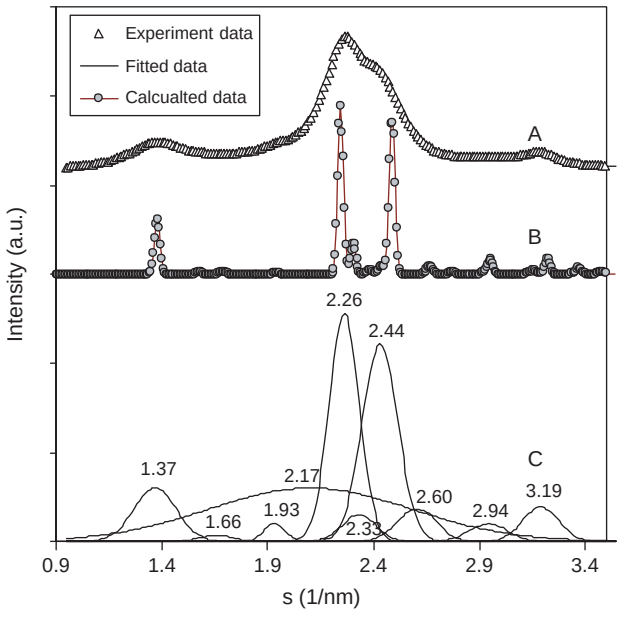

Fig. 4. 1D integrated WAXD intensity profile of sample S3 and corresponding peak deconvolution process to estimate the crystallinity and crystal size. (A) The experimental intensity curve, (B) calculated intensity profile based on the cellulose II structure, (C) the nine crystal reflections and the amorphous background.

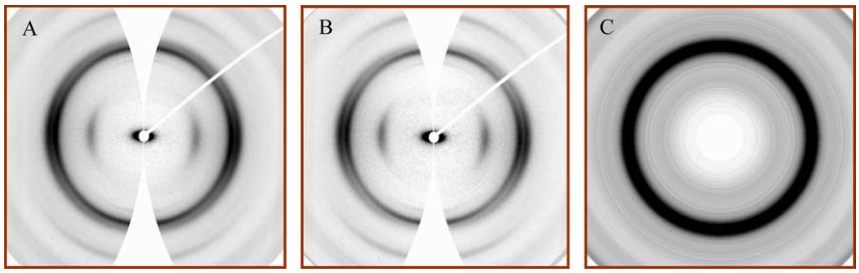

Fig. 5. (A) 2D WAXD pattern after the Fraser correction (sample S3), (B) WAXD pattern of separate anisotropic fraction, (C) WAXD pattern of the residual isotropic fraction.

of the Fraser-corrected 2D WAXD pattern (Fig. 4(A)). Based on the calculated intensity profile from the cellulose II structure (Fig. 4(B)), nine crystal reflection peaks were used in the peak fitting process of the measured intensity profile (Fig. 4(C)). The amorphous peak was obtained from the X-diffraction of ball-milled as-spun cellulose, containing only the amorphous phase. The peak position and intensity of the fitted peaks (Fig. 4(C)) from the measured profile were very similar to those calculated peaks (Fig. 4(B)).

Fig. 5(A) shows the Fraser-corrected 2D WAXD pattern for the S3 sample. The 2D WAXD pattern was separated into two fractions, the isotropic and the anisotropic parts, by using the halo method [39]. The isotropic part includes the scattering from the amorphous phase (and Compton scattering which is usually small in the typical detection angular range and can be ignored). The anisotropic fraction can be further analyzed using the above peak fitting method to determine the oriented crystalline and oriented amorphous phases. Fig. 5(B) and (C) shows the anisotropic (or orientated) fraction and un-orientated (or isotropic) fraction of the WAXD pattern, respectively.

The crystallinity (total and anisotropic fraction) and lateral crystal size (that is related to the crystal fibril diameter) of the regenerated cellulose fibers are listed in Table 2. It was found that the total crystallinity stayed essentially constant (marginal increase from 62 to 64%, well within the experimental accuracy) with the draw ratio in the second coagulation bath (SDR_{II}, 1.08), and also samples S3 (58%) and S4 (62%) showed little variation of the crystallinity. Compared with the results of crystal size in S1, S2 and S4, the crystal size was found to increase with increasing draw ratio in the second coagulation bath. However, the crystal size remained about constant when the draw ratio in the third post-treatment bath was increased. Compared with the two commercial rayon samples, the four regenerated cellulose fibers from the NaOH/thiourea solution exhibited much higher total crystallinity as well as larger crystal size.

With results from S1 and S2 samples, the anisotropic fraction of the crystallinity was found to increase with increasing draw ratio in the second coagulation bath. However, the anisotropic fraction of the crystallinity was found to decrease with increasing draw ratio in the washing and oiling stage, indicating that some oriented crystallites were destroyed by chain pulling during this stage. The change in the crystal size estimated from the anisotropic fraction of the WAXD pattern also supported the above argument. Therefore, the varying wet spinning conditions could affect the crystal structure and orientation of the fiber in different manner. In the second coagulation stage, both crystallinity and crystal size (estimated from total or anisotropic fraction of the 2D WAXD pattern) increased with increasing draw ratio. However, in the third post-treatment bath, the increase in draw ratio might lead to the pull-out of the cellulose chains from the crystal region, resulting in a decrease in the crystallinity and crystal size.

In the oriented cellulose fiber, native or regenerated, the crystal orientation plays an important role and affects the mechanical properties. Table 2 lists Hermans' orientation factor calculated from the (020) reflection in the 2D WAXD patterns. The values of Hermans' orientation factor, $\bar{P}_{2,g}$, of all cellulose fibers spun from the NaOH/thiourea solution were in the range of 0.50–0.60, significantly lower than those of the viscose rayon fibers, which was clearly visible in the WAXD pattern of Fig. 3. All crystal reflections in rayon 1 and rayon 2 were much sharper and more oriented than those in the regenerated samples produced in this study. For rayon 2, the Hermans' orientation parameter was calculated to be about 0.9.

Rather than reducing the orientation distribution to a single parameter $\bar{P}_{2,g}$ as described above, we could also use an empirically chosen explicit $g(\beta)$ function, approximating the observed orientation, for which a calculation of the peak

Table 2
Crystallinity, crystal size and Hermans' orientation factor (estimated from the (020) reflection) of regenerated cellulose fibers estimated from the WAXD data

Samples	Total crystallinity (%)	Crystal size (nm)	Crystallinity of anisotropic part (%)	Crystal size of anisotropic part (nm)	Hermans' orientation factor $\bar{P}_2$
S1	61.8	4.78	67.6	5.30	0.50
S2	63.8	5.25	73.3	5.70	0.55
S3	58.1	5.32	65.7	5.31	0.58
S4	62.3	5.47	65.8	5.87	0.60
Rayon 1	58.4	5.32	63.0	5.46	0.68
Rayon 2	49.1	4.99	55.3	5.00	0.90

profiles in the fiber pattern is computationally feasible, for certain choices of orientation distribution functions even analytically. A preliminary investigation suggests that a modified Onsager [40] distribution (Eq. (1)) may serve for this purpose:

$$g(\beta) = p_0 + (1-p_0)p\cosh(p\cos\beta)/\sinh(p) \quad (1)$$

The introduction of the additional parameter p_0 accounts for the presence of a certain isotropic fraction that appears to be clearly visible in the experimental patterns. The Hermans' orientation factor for this choice of orientation distribution can be given by:

$$\bar{P}_{2,g} = (1-p_0)\{1-3p^{-1}[\coth(p)-p^{-1}]\} \quad (2)$$

Under certain assumptions, which are all well fulfilled in the present case, the peak profile of a peak located (in polar coordinates of the structural unit) at (S_{hkl}, ϕ_{hkl}) is, in good approximation, given by

$$I(s,\phi) = I_{\text{int}}(4\pi s^2 w)^{-1}H[(s-s_{hkl})/w]F(p_0,p,\phi,\phi_{hkl}) \quad (3)$$

where I_{int} is the total integrated peak intensity, H is a 1D normalized peak distribution function of unit integral width, e.g. a Lorentzian function such as $H(s)=(1+\pi^2 s^2)^{-1}$, the peak width in the radial direction is given by w, and F is a function depending on g through an integral transform that can be solved analytically in the present case to produce

$$F(p_0,p,\phi,\phi_{hkl}) = p_0 + (1-p_0)p\cosh(p\cos\phi\cos\phi_{hkl})\, I_0(p\sin\phi\sin\phi_{hkl})/\sinh(p) \quad (4)$$

where I_0 is the modified Bessel function of the first kind of order 0. For the equator peaks, this function reduces to:

$$F(p_0,p,\phi,\pi/2) = p_0 + (1-p_0)pI_0(p\sin\phi)/\sinh(p) \quad (5)$$

Fig. 6(A) and (C) shows calculated fiber diffraction patterns using this model for the sample S1 (Fig. 6(B)) and S4 (Fig. 6(D)). We note that the meridional reflection of (002) appeared to disappear in Fig. 6(A) and (C), because its calculated intensity was very weak compared to the intensities of (110) and (020). The isotropic fraction $p_0=0.35$ and an orientation parameter $p=12$ were used for calculation of Fig. 6(A), and the corresponding $\bar{P}_{2,g}$ was 0.50, which was the same as the $\bar{P}_{2,g}$ of the experimental S1 pattern (Fig. 6(B)). The isotropic fraction $p_0=0.32$ and orientation parameter $p=25$ were used for pattern 6C, leading to a Hermans' parameter $\bar{P}_{2,g}$ of 0.60. A well oriented cellulose II fiber with a very small amount of isotropic fraction ($p_0=0.07$) and $p=95$ corresponding to $\bar{P}_{2,g}=0.90$ (the same as rayon 2) was also calculated and shown in Fig. 6(E). A comparison of the calculated fiber patterns and the experimental patterns in Fig. 6 showed that the calculated WAXD patterns matched the corresponding experimental patterns very closely. The value of isotropic fraction p_0 and orientation parameter p could give some insights on the composition of those new cellulose fibers. For sample S1, the total draw ratio was 0.35 during spinning, resulting in a lower Hermans' orientation factor of about 0.50. Since there was no drawing during wet spinning for S1, the quick flow of the cellulose solution through the spinneret oriented the cellulose molecules along the flow direction. When the draw ratio increased from 1 to 1.14 in the second coagulation stage, the Hermans' orientation factor of sample S4 increased to 0.60. By comparing the isotropic fraction p_0 and the orientation parameter p of Fig. 6(A) with those of Fig. 6(C), the isotropic fraction p_0 decreased, and the orientation parameter p increased, indicating that the isotropic phase decreased during draw at the second coagulation stage and the last washing stage. However, the p_0 decreased only a little bit, from 0.35 to 0.32, and the orientation parameter p increased from 12 to 25, showing that a higher draw ratio during the wet-spinning process mainly increased the orientation by further orienting the already oriented fraction, and not so much by decreasing the isotropic fraction. The isotropic fraction showed only little change during the wet-spinning processing. Rayon 2 exhibited very small p_0 and very large p, in which the isotropic fraction was only 0.07, and it had a relatively higher Hermans' orientation factor of about 0.90.

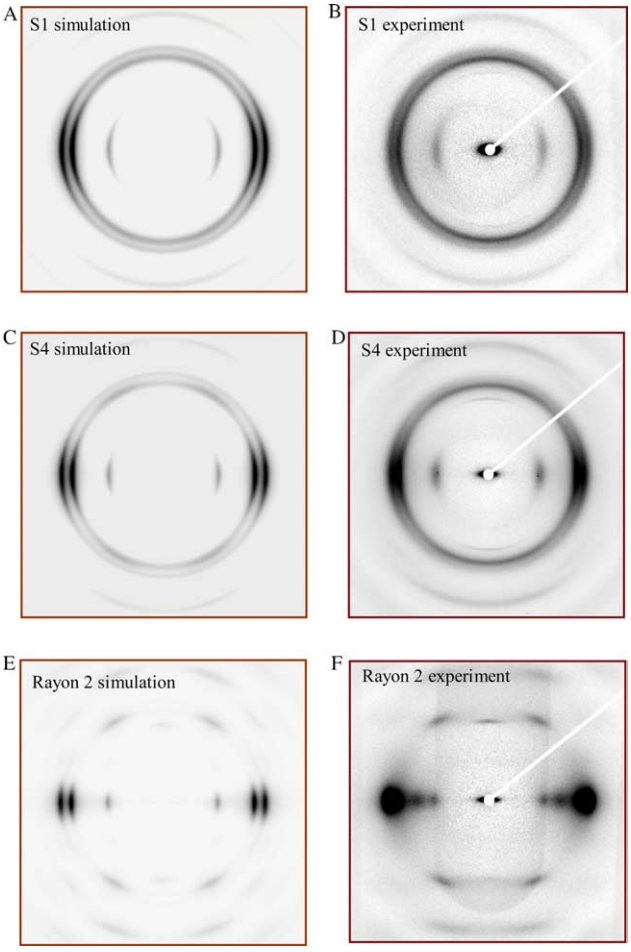

Fig. 6. WAXD patterns of cellulose II fibers from experiment and simulation.

3.2. SAXS results

In 1956, Statton proposed that the diffuse SAXS feature in cellulose fibers could be mainly due to microvoids, where these voids were elongated parallel to the fiber axis, as indicated by

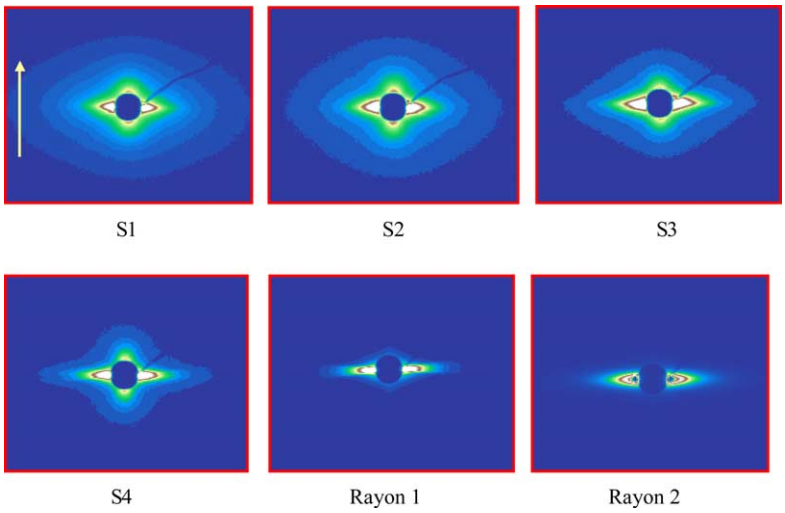

Fig. 7. SAXS patterns of the cellulose fibers (the arrow inset in S1 shows the fiber direction).

the greatest extension of the scattering in the equatorial direction [41]. Hermans, Heikens, and Weidinger investigated the diffuse SAXS pattern of cellulose fibers [42,43], and they found that the expected scattering power from mixed crystalline and amorphous regions was close to the intensity calculated for a volume fraction for a volume fraction of about 1% micorvoids in a solid matrix, which was much lower than the observed scattering power. They quantitatively demonstrated that the observed scattering power in cellulose fibers was much higher than would be expected from mixed crystalline and amorphous regions, in agreement with the intensity calculated for a volume fraction of the order of 1% microvoids in a solid matrix [42,43].

Fig. 7 shows SAXS patterns of regenerated cellulose fibers in this study (Table 1) and the commercial rayon fibers. In all regenerated cellulose fibers, the scattering pattern showed a sharp and elongated equatorial streak superimposed with a relatively weak and short meridian streak. However, only a sharp and elongated equatorial streak was seen in commercial rayon fibers. The equatorial streak could be attributed to the existence of microvoids in cellulose fibers. The amount of microvoids was strongly dependent on the spinning conditions. The elongated shape of the equatorial streak indicated that microvoids were needle-shaped and aligned parallel to the fiber direction. The short meridional scattering streak in the regenerated cellulose fibers suggested the possible existence of a periodic lamellar arrangement between crystalline and amorphous cellulose regions. The long period, L, representing the average distance between the adjacent crystalline lamellae, could be estimated from the position of a meridional scattering maximum. The SAXS intensity profiles of the regenerated cellulose fibers taken along the meridian direction are shown in Fig. 8. A possible meridional maximum appeared to be located inside the beam stop, indicating that the long periods in the regenerated fibers are longer than 100 nm, above the limit of spatial resolution for the SAXS experiment. The S1 sample exhibited the highest intensity among the regenerated cellulose fibers along the meridian direction as seen in Fig. 8. This intensity decreased when the cellulose fiber was drawn in the second coagulation bath and it further decreased after drawing in the third post treatment bath. The decrease in meridional intensity is consistent with the argument discussed above that the crystalline lamellae were destroyed by stretching in the post-treatment bath.

3.3. Structure changes during multi-roller drawing processes

As seen in Fig. 1, the wet spinning process involved multi roller drawing stages (I–III) after several baths: the first coagulation bath (c), a second coagulation bath (d), and the third post-treatment bath (e and f). In each bath, the fiber underwent a stretching process under a specific draw ratio (listed in Table 1). In this study, we only discussed the effect of the draw ratio in the second coagulation stage (d) and the last stage (e and f) on the crystal structure changes of the resulting

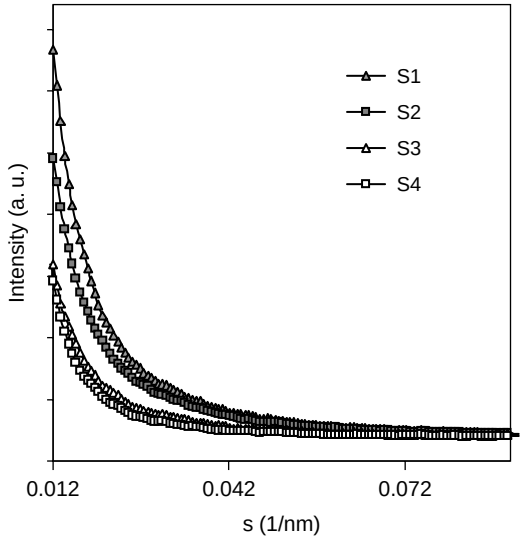

Fig. 8. SAXS intensity profiles of regenerated cellulose fibers along the meridian direction.

cellulose fibers and results have been described in the previous sections.

The exact nature of the processes leading to the formation of oriented lamellar stacks in semi-crystalline cellulose fibers from solution is still a matter of debate and active research. The presence of polar interactions and hydrogen bonds can only further complicate the issue. It is clear that, among other parameters, preferred chain orientation, the presence of aggregates and also chain entanglements can strongly influence the crystallization process. For the time being and in view of the applied nature of this study, carefully correlating these effects in an empirical way with the properties of the resulting fibers appears to be a fruitful approach. However, possible mechanisms about the crystallization process at a molecular level will also be discussed as follows.

3.4. Molecular pathways in wet spinning of cellulose and NaOH/thiourea solution

In order to increase the crystal orientation of regenerated cellulose fibers (and, thus, improve the mechanical properties), we first compared the wet spinning of cellulose in NaOH/thiourea aqueous solution with those by viscose and NMMO (Lyocell) processes. In the viscose process, the regenerated cellulose is obtained by wet spinning of cellulose in xanthate and precipitating in an acidic medium. Recrystallization proceeds only slowly upon precipitation [44]. Therefore, As a result, the fiber properties could be modified by physical means, such as multi roller drawing stages [45]. The recrystallization in Lyocell process is so fast that it is difficult for physical modification after the cellulose solution past the air gap. In the case of the Lyocell process, recrystallization proceeds much faster and leaves only little room for physical modifications. The air gap in the Lyocell process thus becomes very important because it enhances the orientation of cellulose chains in the solution before they reach the coagulation bath [46]. The recrystallization process of cellulose chains in the NaOH/thiourea aqueous solution was also very fast since the neutralization reaction by ion exchange occurs even faster in solution. On the other hand, forming an air gap to spin the cellulose in NaOH/thiourea aqueous solution is difficult because the very high surface tension of the NaOH/thiourea aqueous solution often causes the instability of the extruded fiber, resulting in the formation of disrupted liquid droplets on the spinneret. As the solution stream submerges in the coagulation bath, the fast sol–gel transition (due to the rapid hydrogen bond formation) can also limit the possibilities for post-physical modifications, as shown by WAXD/SAXS results in this study. For example, the crystallinity and crystal orientation of the cellulose fiber did not show a significant increase from S1 to S4.

The flow orientation of polymer chains in the solution or melting state was thoroughly discussed by Keller and Kolnaar [47,48]. The flow orientation of cellulose chains in solution as it passes through a spinneret that generates a high shear rate could provide a possible means to increase the orientation of cellulose chains before it reaches the coagulation bath. A liquid gap configuration similar to the air gap in Lyocell process could also provide a possible pathway to increase the orientation of cellulose chains.

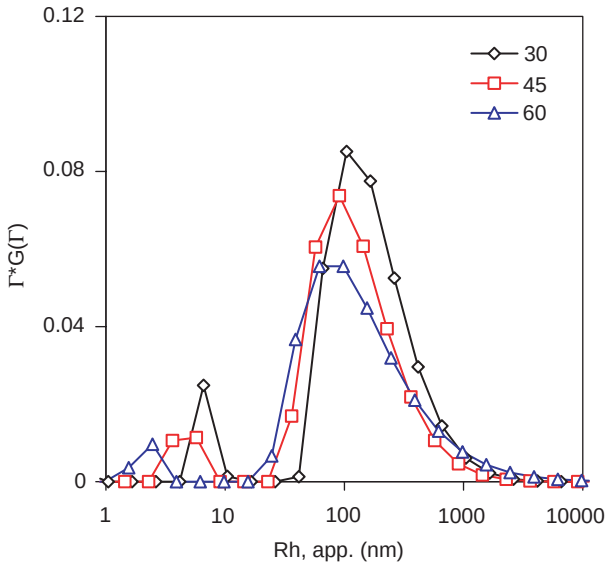

Fig. 9. CONTIN analysis of DLS measurements on cellulose and NaOH/thiourea aqueous solutions.

We speculate that in wet spinning of cellulose in NaOH/thiourea solutions, a certain degree of aggregation would be helpful because it increases the effective molecular weight. Therefore, the drawablility of the cellulose solution can increase. The aggregation of cellulose in NaOH/thiourea solution was studied by dynamic light scattering. Fig. 9 shows a typical apparent hydrodynamic radius distribution as obtained by the CONTIN analysis of the DLS measurements of cellulose solution at different concentrations in the dilute solution regime. The dominant peaks at $R_h = 128$ nm represented the aggregates of cellulose molecules in NaOH/thiourea aqueous solution. The cellulose aggregates in NaOH/thiourea aqueous solution were found to be similar to those in NaOH/urea aqueous solution ($R_h \sim 170$ nm, $R_g \sim 270$ nm, detailed results will be published elsewhere). Morgenstern and Roder et al. [49,50] also reported that R_g was about 266 nm in viscose with cellulose of similar molecular weight. Thus, the NaOH/thiourea system showed good promise as a more environmentally friendly solvent for cellulose, as suggested by Zhang et al. [6,7], even though cellulose could not be truly dissolved at a molecular level. Compared with the cellulose concentration in viscose and Lyocell processes (both close or higher than 10 wt%), the cellulose concentration in NaOH/thiourea solution was relatively low (4.8 wt%). Thus, the stress applied to the polymer chains by flow would relax faster due to the lower entanglements of polymer chains. The rapidly relaxed stress would decrease the orientation of cellulose chains, leading to shrinkage of the swollen cellulose fiber in the coagulation bath. Therefore, the concentration of the cellulose should be increased to reach a higher flow orientation of the cellulose chains during spinning. Yamashiki et al. studied the wet spinning process of gelatinized cellulose dopes prepared from alkali solution [51]. They found that the shear stress

imposed on the gelatinized dope, when extruded into a coagulation bath, significantly affected the mechanical properties of the regenerated cellulose fibers. The pre-gelation of the cellulose in NaOH/thiourea solution before it reaches the coagulation bath would, to some extent, also decrease the fast stress relaxation and, thus, improve the drawablility of the solution in the coagulation bath, which will be the subject of future study.

The effect of the coagulant component on the spinnability of cellulose in NaOH/thiourea solution was also studied by Zhang et al. [7]. The different coagulants exhibited different coagulation rates, which would affect the recrystallization rates in the coagulation bath. A careful selection of the coagulant and the length of the first and second coagulation bath could also increase the draw ratio in both coagulation baths and, thus, enhance both crystallinity and crystal orientation. The last draw stage can also increase the orientation of the cellulose fiber; however, it can also decrease the crystallinity. Thus, a systematic design of the multi-roller draw spinning process is needed to improve the current process of producing regenerated cellulose fibers from the NaOH/thiourea solutions.

4. Conclusions

Cotton linter pulp was dissolved in NaOH (9.5 wt%)/thiourea (4.5 wt%) aqueous solutions and was wet spun by using a multi-roller drawing process to obtain regenerated cellulose fibers. The structure of the regenerated cellulose fibers was studied by using synchrotron WAXD and SAXS techniques. The initial chosen spinning configuration produced regenerated cellulose fibers with higher crystallinity, but lower orientation, than those of commercial rayon fibers produced by the viscose process. Further improvements are expected. SAXS results showed that a meridional scattering streak was present in all regenerated cellulose fibers from the NaOH/thiourea solutions, suggesting an oriented lamellar structure with long period larger than 100 nm in the fibers. The crystallinity and orientation of the cellulose fiber did not show a significant increase from S1 to S4. This suggests that the recrystallization process of cellulose in the NaOH/thiourea aqueous solution was faster and left only little room for physical modification of crystal structure such as multi-roller drawing. Improvements of flow orientation of cellulose aggregates in the solvent before reaching the coagulation bath, and reduction of the recrystallization rate (or hydrogen bonding formation rate) during coagulation during drawing might be two effective pathways to enhance the chain orientation in the regenerated cellulose fibers in the current wet spinning process of NaOH/thiourea solutions. Overall, the low cost and low toxicity of the new solvent system by wet spinning process appear quite promising for the development of an economical and environmentally friendlier process for the regeneration of cellulose fibers.

Acknowledgements

The financial support of this work was provided by the Department of Energy (DEFG0286ER45237.022 and DEFG0299ER45760), the Office of Naval Research (N000140310932) and the National Science Foundation (DMR0454887 and DMR0405432), and supported by High-Technology Research and Development Program of China (2003AA333040) and the Major Grant of the National Natural Science Foundation of China (59933070).

References

[1] Fink HP, Weigel P, Purz HJ, Ganster J. Prog Polym Sci 2001;26:1473.
[2] Zugenmaier PJ. Prog Polym Sci 2001;26:1341.
[3] Philipp B. J Macromol Sci, Pure Appl Chem 1993;A30:703.
[4] Rosenau T, Potthast A, Sizta H, Kosma P. Prog Polym Sci 2001;26:1743.
[5] Zhou J, Zhang L. Polym J 2000;32:866.
[6] Zhang L, Ruan D, Zhou J. Ind Eng Chem Res 2001;40:5923.
[7] (a) Ruan D, Zhang L, Zhou J, Jin H, Chen H. Macromol Biosci 2004;4:1105.
(b) Zhang L, Cai J, Zhou J. Chinese patent ZL 03128386.1; 2005.
(c) Ruan D, Lv A, Zhou J, Zhang L, Chen H, Chen X, et al. Private communication.
[8] Cai J, Zhang L, Zhou J, Li H, Chen H, Jin H. Macromol Rapid Commun 2004;25:1558.
[9] Zhang L, Ruan D, Gao S. J Polym Sci, Part B: Polym Phys 2002;40:1521.
[10] Weng L, Zhang L, Ruan D, Shi L, Xu J. Langmuir 2004;20:2086.
[11] Zhou J, Zhang L, Cai J. J Polym Sci, Part B: Polym Phys 2004;42:347.
[12] Zhou J, Zhang L, Deng Q, Wu X. J Polym Sci, Part B: Polym Phys 2004;42:5911.
[13] Chen Y, Zhang L. J Appl Polym Sci 2004;94:748.
[14] Ruan D, Zhang L, Mao Y, Zeng M, Li X. J Membr Sci 2004;241:265.
[15] Cai J, Zhang L. Macromol Biosci 2005;5:539.
[16] Zhang L, Mao Y, Zhou J, Cai J. Ind Eng Chem Res 2005;44:522.
[17] Nishikawa S, Ono S. Proc Tokyo Math Phys Soc 1913;7:131.
[18] Hermans PH. Physics and chemistry of cellulose fibres. New York: Elsevier Publishing Co.; 1949.
[19] Roelofsen PA. The plant cell-wall. Berlin, Germany: Gebröder Borntraeger; 1959.
[20] Chu B, Hsiao BS. Chem Rev 2001;101(6):1727.
[21] Hsiao BS, Kennedy AD, Leach RA, Chu B, Harney P. J Appl Crystallogr 1997;30:1084.
[22] Chen X, Burger C, Wang X, He W, Yoon K, Somani RH, et al. PMSE Prepr 2005;93:751.
[23] Kelarakis A, Yoon K, Somani RH, Chen X, Hsiao BS, Chu B. Polymer 2005;46:11591.
[24] Hsiao BS, Sauer BB, Verma RK, Zachmann HG, Seifert S, Chu B, et al. Macromolecules 1995;28:6931.
[25] Ran S, Cruz S, Zong X, Fang D, Chu B, Hsiao BS. Adv X-Ray Anal 2000;43:344.
[26] Liu L, Wan Q, Liu T, Hsiao BS, Chu B. Langmuir 2002;18:10402.
[27] Chen X, Yoon K, Burger C, Sics I, Fang D, Hsiao BS, et al. Macromolecules 2005;38:3883.
[28] Hsiao BS, Yang L, Somani RH, Avila-Orta CA, Zhu L. Phys Rev Lett 2005;94:117802.
[29] Ran S, Wang Z, Burger C, Chu B, Hsiao BS. Macromolecules 2002;35:10102.
[30] Chu B. Laser light scattering. 2nd ed. New York: Academic Press; 1991.
[31] Zugenmaier P. Prog Polym Sci 2001;26:1341.
[32] Stipanovic A, Sarko A. Macromolecules 1976;9:851.
[33] Kolpak KJ, Blackwell J. Macromolecules 1976;9:273.
[34] Dudley RL, Fyfe CA, Stephenson PJ, Deslandes Y, Hamer GK, Marchessault RH. J Am Chem Soc 1983;105:2469.
[35] Isogai A, Usuda M, Kato T, Uryu T, Atalla RH. Macromolecules 1989;22:3168.
[36] Gessler K, Krauss N, Steiner T, Betzel C, Sandman C, Saenger W. Science 1994;266:1027.
[37] Raymond S, Heyraud A, Tran Qui D, Kvick A, Chanzy H. Macromolecules 1995;28:2096.

[38] Langan P, Nishiyama Y, Chanzy H. Biomacromolecules 2001;2:410.
[39] Ran S, Zong X, Fang D, Hsiao BS, Chu B. Macromolecules 2001;34: 2569.
[40] Onsager L. Ann NY Acad Sci 1949;51(4):627.
[41] Hermans PH, Heikens D, Weidinger A. J Polym Sci 1959;35:145.
[42] Statton WO. J Polym Sci 1956;32:395.
[43] Heikens D. J Polym Sci 1959;35:139.
[44] Iovleva MM, Papkov SP. Sov Beitr Faserforschg Textilchem 1968;5:300.
[45] Jayme G, Balser K. Pure Appl Chem 1967;14:395.
[46] Mortimer SA, Pecuy AA. J Appl Polym Sci 1996;60:1747.
[47] Keller A, Kolnaar HWH. Flow-induced orientation and structure formation. In: Cahn RW, Hassen P, Kramer EJ, editors. Materials science and technology. Germany: VCH Verlagsgesellschaft mbH; 1997 [chapter 4].
[48] Keller A, Odell JA. Colloid Polym Sci 1985;263:181.
[49] Morgenstern B, Röder T. Papier 1998;52:713.
[50] Roder T. PhD Thesis. Technical University of Dresdenl; 1998.
[51] Yamashiki T, Saitoh M, Yasuda K, Okajima K, Kamide K. Cellul Chem Technol 1990;24:237.